ORIGINAL ARTICLE

sciendo

10.2478/AMB-2024-0062

MOLECULAR INSIGHTS ON BINDING INTERACTIONS OF CYCLOOXYGENASE AND LIPOXYGENASE ACTIVITIES ON MALONDIALDEHYDE IN NAPHTHALENE-EXPOSED WISTAR RATS

I. Olaoye[1], G. Akhigbe[2], A. Awotula[1], B. Oso[1], O. Agboola[1], A. Adebayo[1], R. Banwo[1]

[1]Department of Biochemistry and Molecular Biology, McPherson University-Seriki Sotayo, Nigeria
[2]Department of Chemical Sciences, McPherson University – Seriki Sotayo, Nigeria

Abstract. Background. *Naphthalene (NA), a polycyclic aromatic hydrocarbon, is an environmental pollutant from different sources exhibiting toxicities via free radical generation. However, NA has been used in the industry as surfactants, solvents, resins, and in medicine – as an anti-viral, anti-bacterial, and antiinflammatory drug. Malondialdehyde (MDA), a by-product in lipid peroxidation and prostaglandin synthesis, is a biomarker in lipid peroxidation evaluation and cyclooxygenase (COX) and lipoxygenase (LOX) activities assessment via inhibition.* ***Results.*** *The twenty-four adult male Wistar rats were randomly divided into six groups of four rats each. The animals in the control groups were given food and water only while the NA-exposed groups: group 3 (N1) rats exposed to NA at 0.75 mg/m^3 for 2 hours, group 4 (N2) rats exposed to NA at 1.5 mg/m^3 for 2 hours, group 5 (N3) rats exposed to NA at 0.75 mg/m3 for 4 hours and group 6 (N4) rats exposed to NA at 1.5 mg/m^3 for 4 hours. In addition, in silico work was carried out on the homologs of COX and LOX with NA and its selected metabolites. The in vivo result revealed a significant increase (7.50 ± 0.29) in MDA synthesis at the lower dose (0.75 g/m^3) during the 2 hrs exposure time compared to the control while the higher dose (1.50 g/m^3) showed a significant reduction in MDA level (1.00 ± 0.01) compared to the control. Furthermore, docking result depicted highest binding score for 1-nitronaphthalene towards COX and LOX.* ***Conclusions.*** *This study suggested that NA could reduce the synthesis of MDA in the in vivo work, and 1-nitronaphthalene showed the highest binding affinity in the in silico work.*

Key words: *naphthalene, malondialdehyde, cyclooxygenase, lipoxygenase, 1-nitronaphthalene*

Corresponding authors: *Babatunde Oso, basjoe08@gmail.com, Olubukola Agboola, bkbakanni@gmail.com*

Received: *12 November 2023;* ***Accepted:*** *20 March 2024*

BACKGROUND

Humans are at risk of environmental pollutants due to constant exposure to different contaminants and toxins from different sources. Naphthalene (NA) is a simple polycyclic aromatic hydrocarbons ubiquitous aryl compound with high solubility but toxic. The route of human exposure to NA could be ingestion, inhalation and dermal adsorption. As a result of its complex nature, when it's inhaled, it tends to cause irritation, as well as bio-accumulate/magnify in the food chain, which can have adverse

effects on human health such as pulmonary, hematologic and ocular damage [1, 2].

However, NA has been found useful industrially in manufacturing leather tanning agents, dyes, resins, pesticides, moth repellents, surfactants, solvents and deodorants [3]. It has also been used in anti-viral, anti-bacterial, anti-cancer, and anti-inflammatory agents, amongst others [4, 5, 6]. Also, Pandya et al. [5] reported the nonsteroidal anti-inflammatory properties of NA, which can inhibit cyclooxygenase (COX-1 and COX-2). Inflammation in organisms occurs as a protective response by vascular tissues to harmful/injurious stimuli, leading to tissue healing as the response defends the host by getting rid of the cause of injury [7]. Malondialdehyde (MDA) is produced as a result of lipid peroxidation in the cell membrane and has been used as an index for cyclooxygenase (COX) and lipoxygenase (LOX) activities, as well as a biomarker for lipid peroxidation in vivo [8, 9]. The inhibition of COX and LOX invariably hinders the release of MDA as a by-product during prostaglandin synthesis in the blood platelets and other cells, such as liver cells, via endoperoxidase. Hence, the regulation of the production of COX and LOX can serve as a good analgesic agent. This study assessed the analgesic properties of NA on COX and LOX activities via MDA synthesis in NA-exposed Wistar rats.

METHODS

NA was purchased from Loba Chemie Laboratory Reagents and fine chemicals, India. Thiobarbituric acid (TBA), Trichloroacetic acid (TCA) and glacial acetic acid 99% pure were purchased from BDH (BDH, England) and twenty-four male Wistar Rats.

Animal Grouping and MDA Assay (In vivo Study)

The adult male Wistar rats with an average weight of 212.50 g used in this study were purchased from the animal house, Department of Physiology, University of Ibadan, Oyo State, Nigeria. The animals were allowed to acclimatize for two weeks in ventilated cages at room temperature (28-30 ºC) before the experiment. All experimental procedures were carried out in accordance with the NIH Guidelines for the care and use of Laboratory Animals. Twenty-four Wistar rats of 2-3 months old were randomly divided into six groups of four rats each. Group 1 (Control 1) and group 2 (Control 2) rats were given food and water only, group 3 (N1) rats were exposed to NA at 0.75 mg/m^3 for 2 hours, group 4 (N2) rats were exposed to NA at 1.5 mg/m^3 for 2 hours, group 5 (N3) rats were exposed to NA at 0.75 mg/m^3 for 4 hours and group 6 (N4) rats were exposed to NA at 1.5 mg/m^3 for 4 hours. The animals were given standard laboratory chow and water ad libitum, except when exposed to NA vapor for 14 days. The rats were sacrificed 24 hours after the last hour of NA exposure and an overnight fast. The blood sample was collected into a plain bottle and centrifuged at 650 g for 5 minutes, and the serum was separated from the blood cells. The serum samples were kept in the freezer (-20 ºC) for MDA analysis.

The MDA assessment was done using the method described by Buege and Aust [10]. Exactly 2 ml of TCA-TBA-HCl reagent (0.37% thiobarbituric acid, 0.24 N HCl and 15% trichloro acetic acid in 1:1:1) was added to 1.0 ml of the sample and boiled at 100 °C for 15 min. The mixture was allowed to cool, centrifuged at 3,000 g for 15 minutes and the supernatant was removed. The absorbance of the supernatant was read against the reagent blank at 532 nm.

$$MDA = ((Abs \times TV)) / ((\varepsilon \times SV))$$

ε of MDA-TBA complex = 1.56 105 M^{-1} cm^{-1}

Where, Abs = absorbance, TV = total volume, SV = sample volume, ε = molar extinction

Statistical analysis

The obtained results were expressed as mean ± standard deviation of four determinations and analyzed using one-way analysis of variance (ANOVA) for mean differences between different doses followed by Duncan post hoc correlation.

In silico Study

In addition to the in vivo MDA biochemical assay, the *in silico* study was done to assess the molecular mechanism interaction via the binding affinity prediction of cycloxygenase (COX) and lipoxygenase (LOX) active sites to NA and its metabolites as well as indomethacin (known inhibitor for COX and LOX). The structurally characterized Rattus norvegicus COX and LOX-modeled proteins and ligands were converted to the dockable pdbqt format using Autodock tools. The pdbqt format of the proteins, as well as those of the ligands, was dragged into their respective columns, and the software was run. Blind docking of the ligands to the protein target was done, and binding scores were determined using PyRx-Python Prescription 0.8 (The Scripps Research Institute) [11]. The dimensions were set as grid center: x = -16.9178, y = -41.3417, z = -28.4564 and size: x = 95.0774, y = 70.4855, z = 92.4516 for COX and center: x = 23.8698, y = 39.2749, z = 39.6342 and size: x = 98.7109, y = 106.3529, z = 99.6213 for LOX. The binding scores of NA and its selected metabolites are compared to the binding score of indomethacin. The first three ranking binding score results for all the ligands towards COX and LOX model obtained were

selected and subjected to statistical analysis to see any significant difference among the COX model-ligand and LOX model-ligand interactions. The obtained statistical results were expressed as mean ± standard deviation of three determinations, analyzed using one-way analysis of variance (ANOVA) for mean differences between different ligands followed by Duncan post hoc correlation. The obtained autodocked files for all the ligands and the respective autodocked COX and LOX models were visualized using Discovery Studio BIOVIA 2020, and the interaction views were presented in 2D and 3D.

Ligands and Protein Preparation

The three-dimensional (3D) SDF structures of NA (CID: 931), its metabolites (such as 1-nitronaphthalene (CID: 6849), 1-methylnaphthalene (CID: 7002), 1,2-naphthoquinone (CID: 10667), and indomethacin (CID: 3175) were retrieved from PubChem database (www.pubchem.ncbi.nlm.nih.gov) [12]. The rat primary sequence of COX and LOX with UniProtKD ID: P35355 and P12527 were retrieved from the UniProt database (https://www.uniprot.org/) [13]. The structural characterization of Rattus norvegicus COX and LOX sequences was done using the Swiss model webserver to obtain their 3D structures (https://swiss-model.expasy.org/interactive/) [14] while the quality of the modeled structure was checked using online PROCHECK webserver (https://saves.mbi.ucla.edu/) [15, 16].

Molecular simulation

The obtained auto-docked files for all the ligands and the auto-docked COX and LOX models were converted to PDB format using Discovery Studio BIOVIA 2020. Each PDB file of all the ligands was combined separately with the COX and LOX model PDB files using PyMOL as a molecule for molecular dynamic simulations. The retrieved HETATMs of the respective combinations were pasted in the prodrug online web server (http://davapc1.bioch.dundee.ac.uk/cgi-bin/prodrg/submit.html) for GROMOS topology in ZIP format as ligands [17]. The respective prepared molecules (PDB files) and ligands (ZIP files) were uploaded into the simlab online web server (https://simlab.uams.edu/ProteinWithLigand/protein_with_ligand.html) [18, 19] for the molecular simulation using the server default settings.

RESULTS

The in-vivo result of the study showed a significant increase in the serum MDA level of both doses of NA 2 hrs exposure in Wistar rats compared to the control. However, the serum MDA level decreased significantly in a dose-dependent manner compared to control in the 4 hrs of NA exposure (Table 1).

Table 1. Effects of naphthalene exposure in the serum of male Wistar rats on MDA synthesis

GROUPS	MDA (2 hrs)	MDA (4 hrs)
Control	4.50 ± 0.87^{a}	7.25 ± 0.63^{a}
0.75 g/m^3	7.50 ± 0.29^{b}	5.75 ± 0.75^{b}
1.50 g/m^3	4.75 ± 0.25^{c}	1.00 ± 0.01^{c}

Different superscript indicates significant differences at $P < 0.05$

i ii

Fig. 1. The 3D Swiss model crystal structures of COX and LOX

The swiss model of rat COX and LOX showed GMQE scores of 0.95 and 0.88, respectively, while -1.02 and -0.57 were obtained, respectively for QMEAN scores using arachidonate 5-lipoxygenase (PDB ID: 3V92; resolution 2.74 Å for COX) and prostaglandin G/H synthase-2 (PDB ID: 5F19; resolution 2.04 Å for LOX) as template for the modeling (Figure 1). In addition, 90.9% and 91.9% values for residues in the favored region were obtained for COX and LOX, respectively, using PROCHECK (Figures 2 and 3).

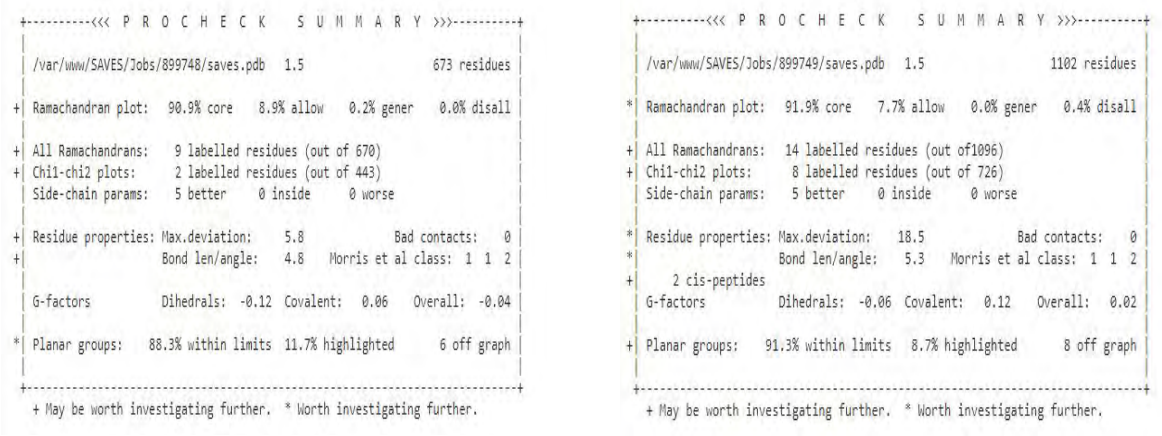

i ii

Fig. 2. The PROCHECK summary of 3D Swiss model COX and LOX crystal structures

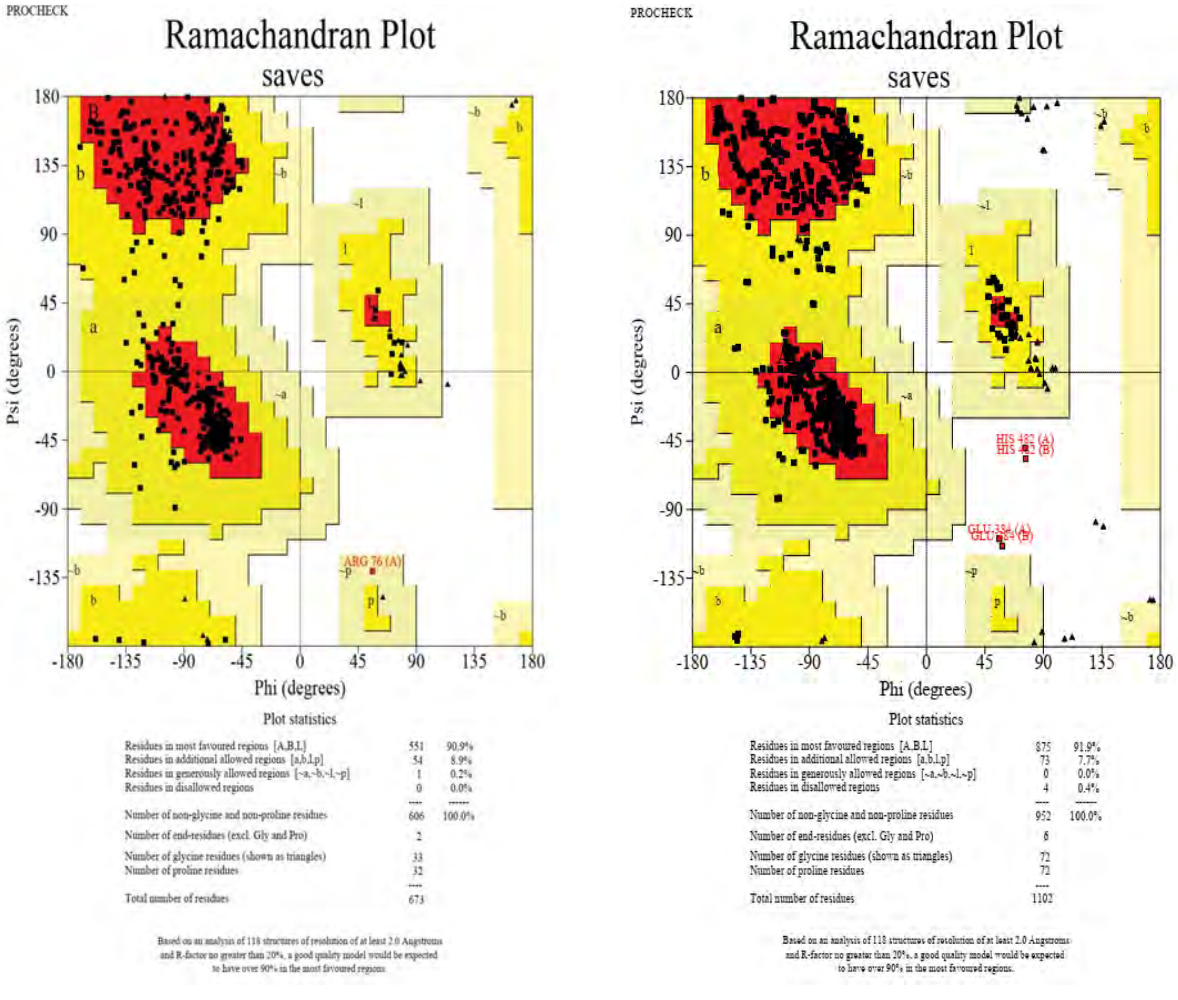

i ii

Fig. 3. The PROCHECK Ramachandran plots of COX and LOX

The result of the theoretically characterized models of COX in this study showed that all the ligands assessed have lower binding scores compared to indomethacin. However, the indomethacin binding score is not significantly different from 1-nitronaphthalene and 1-methylnaphthalene (Table 2) (Figures 4a and 4b). Also, in an almost similar pattern, 1-nitronaphthalene depicted the best binding score among the ligands (Table 3) (Figures 5a and 5b).

The molecular simulation of COX and LOX by the ligands investigated considering radii of gyration, root mean square deviation, root mean square fluctuation and solvent accessible surface area as factors.

Table 2. Molecular docking binding scores of naphthalene and its metabolites towards COX

Ligand/CIDs	COX Binding Score (Kcal/mol)	Interacting Residues
Naphthalene (931)	-6.40 ± 0.00^{ab}	Met231, Tyr234, Lys656
1-nitronaphthalene (6849)	-7.07 ± 0.38^{c}	Met231, Tyr234, Lys656, Leu657
1-methylnaphthalene (7002)	-6.87 ± 0.06^{bc}	Met231, Tyr234, Lys656
1,2-naphthoquinone (10667)	-6.23 ± 0.32^{a}	Cys99, Arg101, Asp166
Indomethacin (3175)	-7.00 ± 0.36^{c}	Val243, Leu244, Lys246, Arg370, Ala453

Different superscript indicates significant differences at P < 0.05

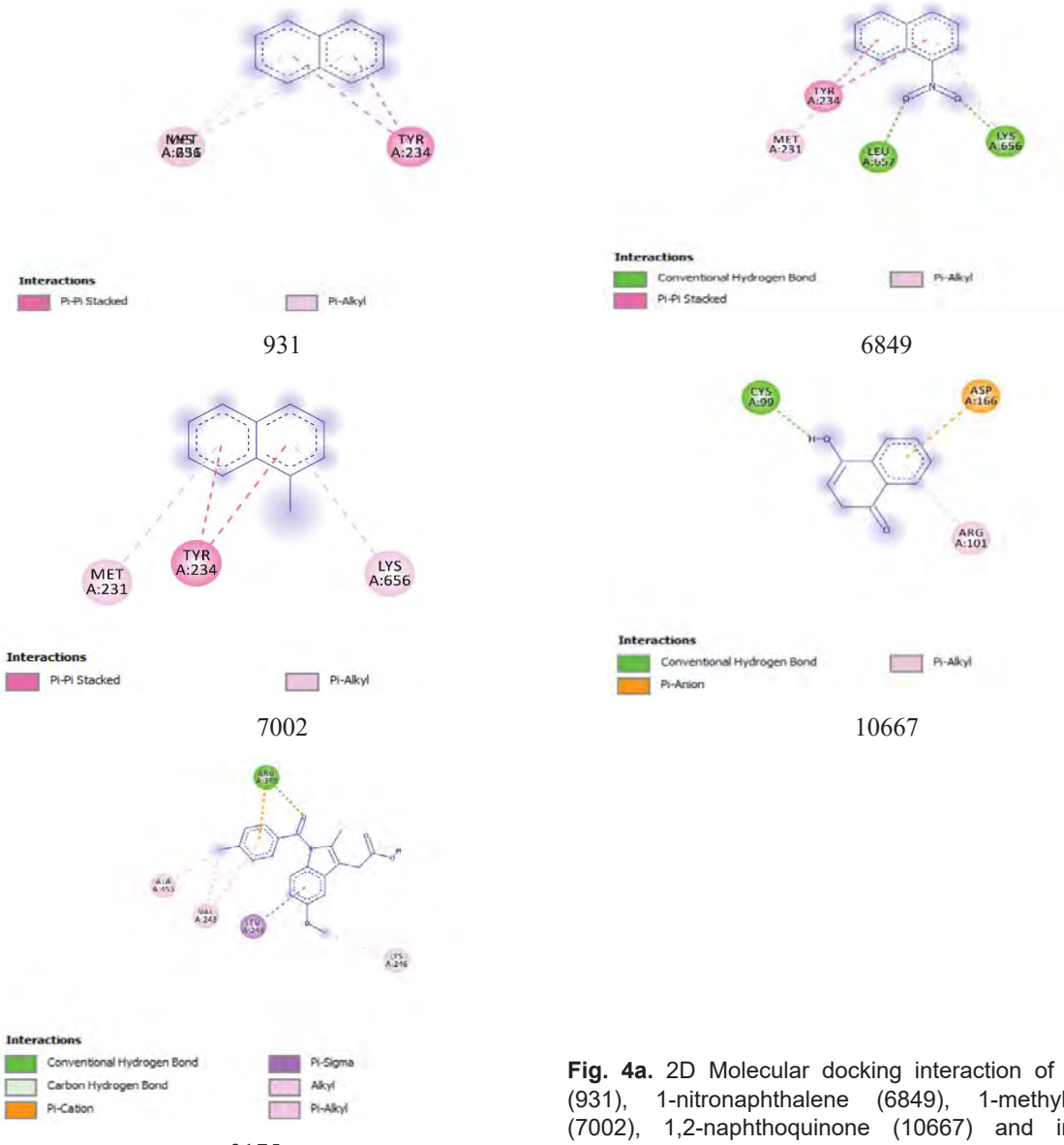

Fig. 4a. 2D Molecular docking interaction of naphthalene (931), 1-nitronaphthalene (6849), 1-methylnaphthalene (7002), 1,2-naphthoquinone (10667) and indomethacin (3175) towards modeled COX

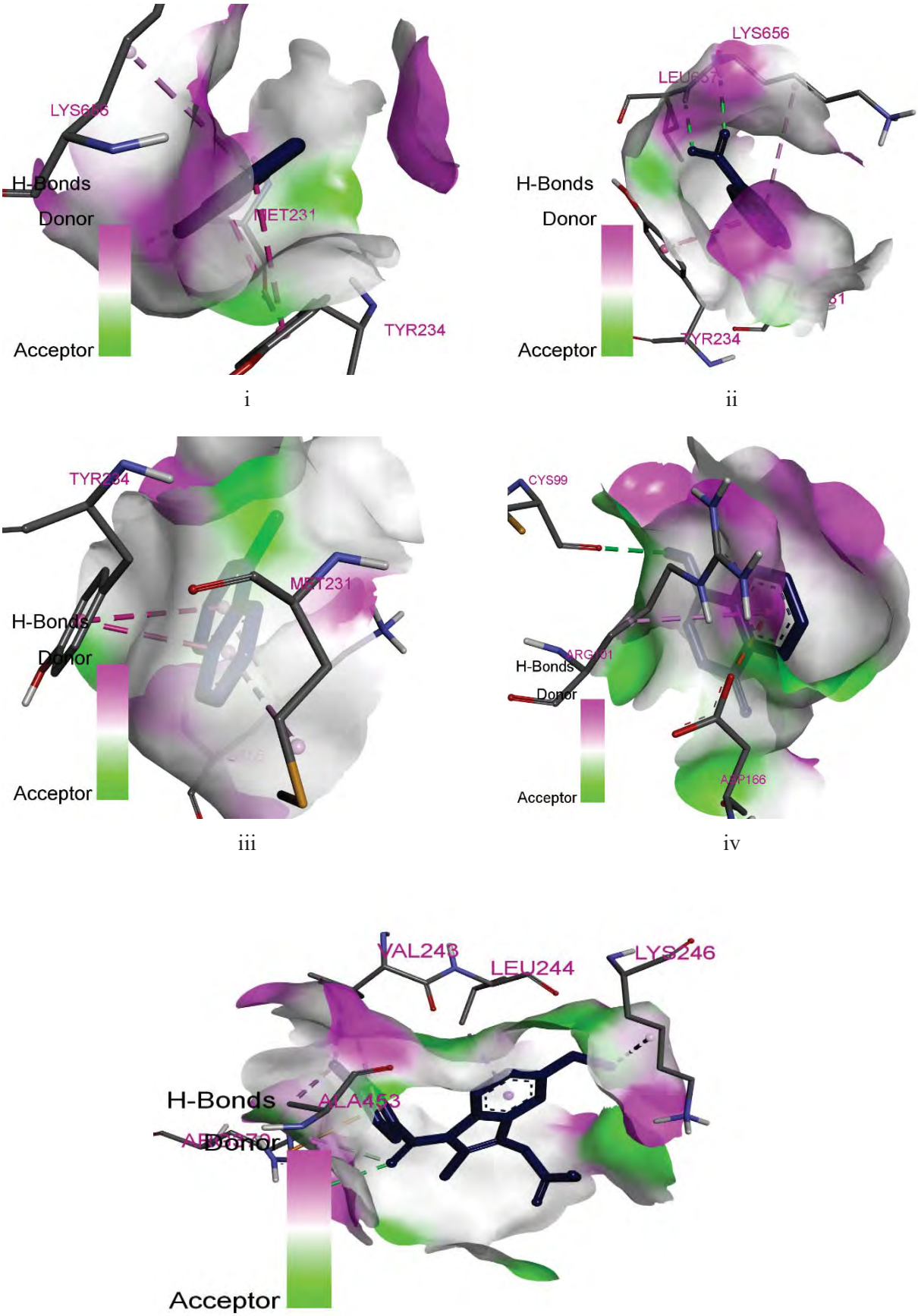

Fig. 4b. 3D Molecular docking interaction of naphthalene (931), 1-nitronaphthalene (6849), 1-methylnaphthalene (7002), 1,2-naphthoquinone (10667) and indomethacin (3175) towards modeled COX

Table 3. Molecular docking binding scores of naphthalene and its metabolites towards LOX

Ligand CIDs	LOX Binding Score (Kcal/mol)	Interacting Residues
Naphthalene (931)	-6.56 ± 0.32[a]	Val335, Leu338, Trp373, Met508, Val509
1-nitronaphthalene (6849)	-7.03 ± 0.32[ab]	Ala188, Gln189, His193, His374
1-methylnaphthalene (7002)	-6.50 ± 0.69[a]	Ala188, Gln189, His374
1,2-naphthoquinone (10667)	-6.47 ± 0.29[a]	Asn24, Leu138, Arg455
Indomethacin (3175)	-7.63 ± 0.42[b]	Leu131, Leu210, Gly221, Leu224, Gln227, Arg314

Different superscript indicates significant differences at P < 0.05

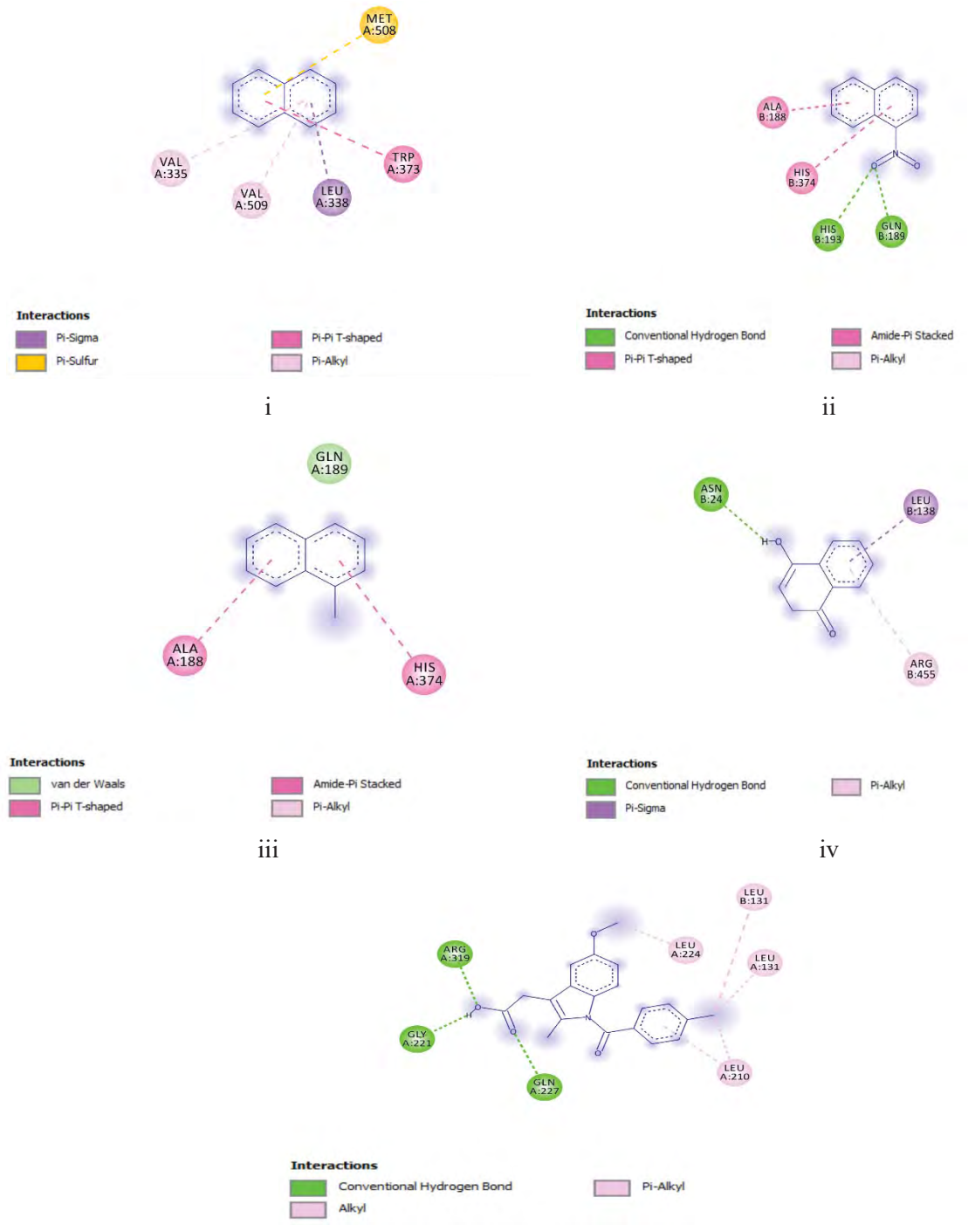

Fig. 5a. 2D Molecular docking interaction of naphthalene (931), 1-nitronaphthalene (6849), 1-methylnaphthalene (7002), 1,2-naphthoquinone (10667) and indomethacin (3175) towards modeled LOX

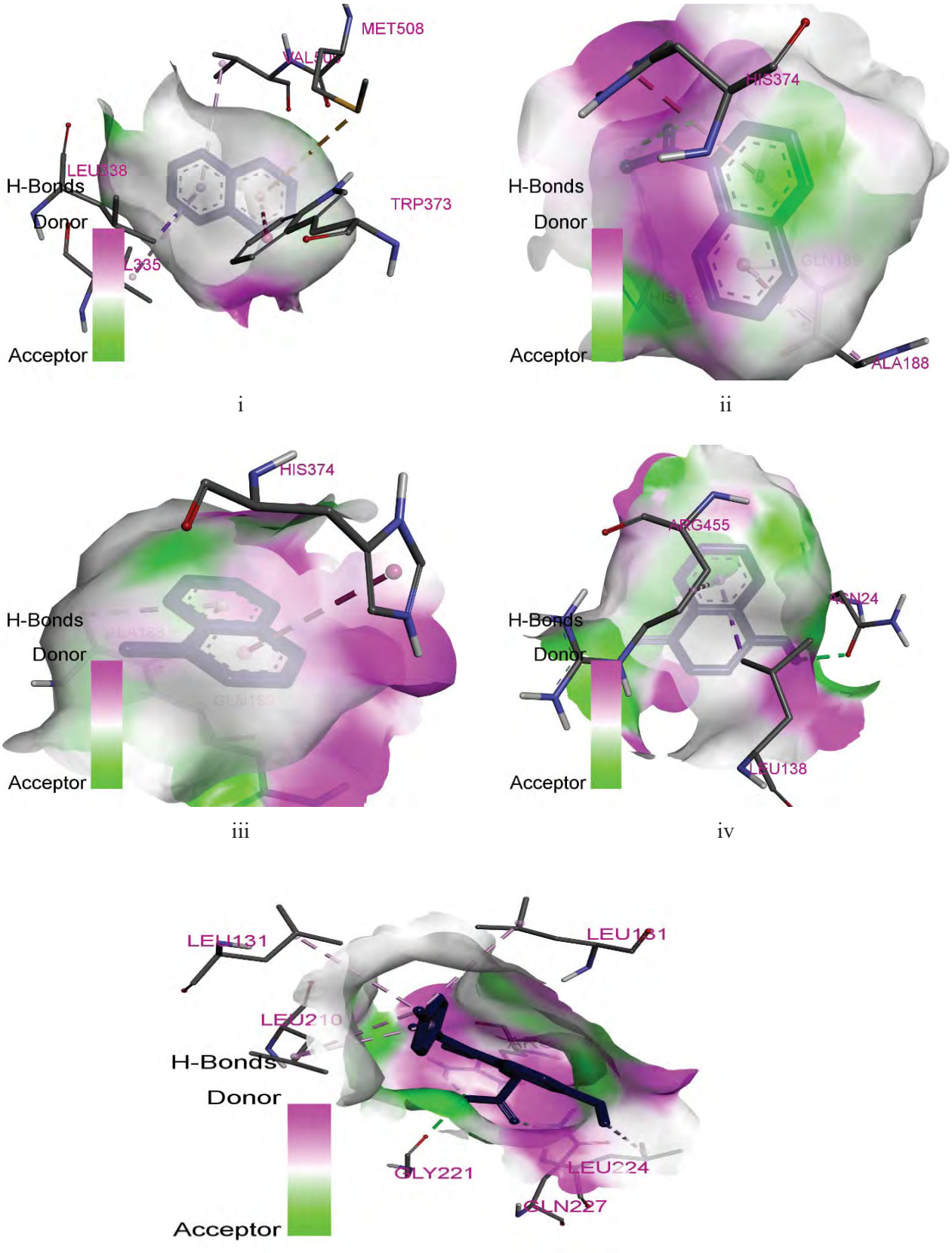

Fig. 5b. 3D Molecular docking interaction of naphthalene (931), 1-nitronaphthalene (6849), 1-methylnaphthalene (7002), 1,2-naphthoquinone (10667) and indomethacin (3175) towards modeled LOX

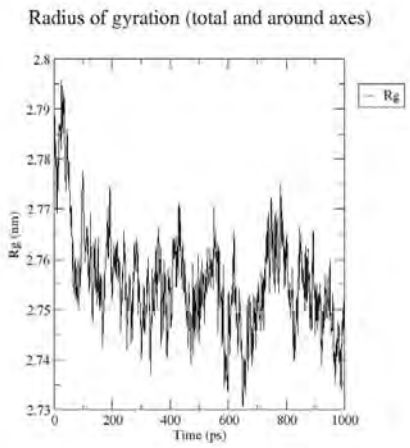

931

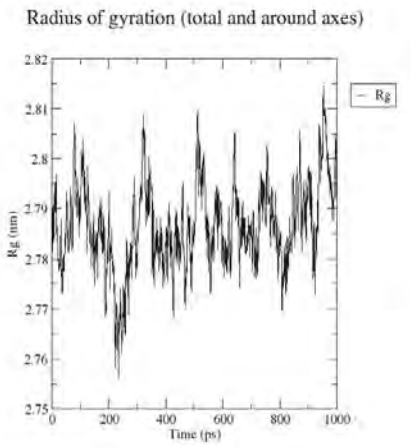

6849

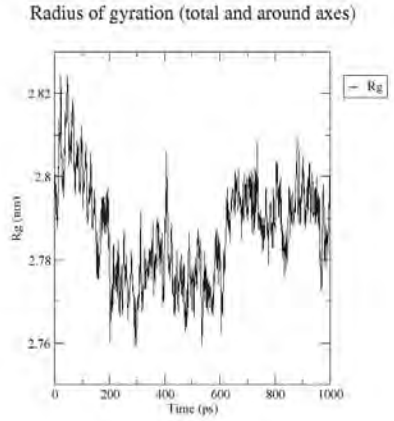

7002

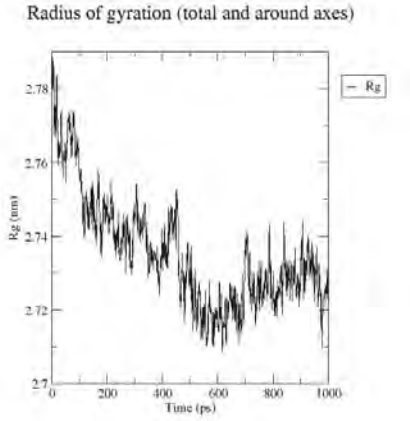

10667

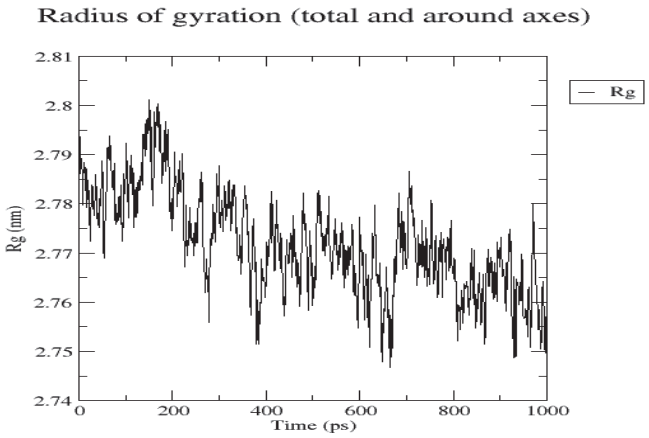

3175

Fig. 6a. Molecular dynamics simulation showing the Radius of gyration of Naphthalene, 1-nitronaphthalene, 1-methylnaphthalene, 1,2-naphthoquinone and indomethacin towards COX

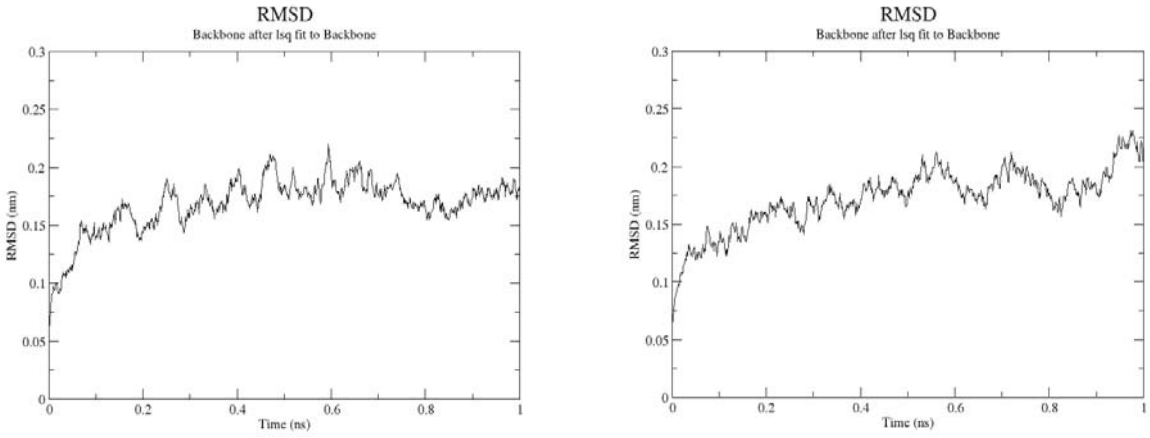

931

6849

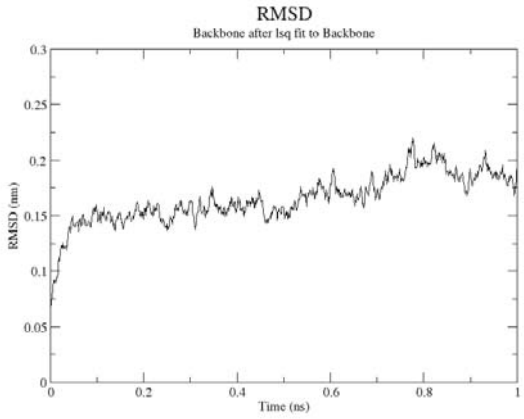

7002

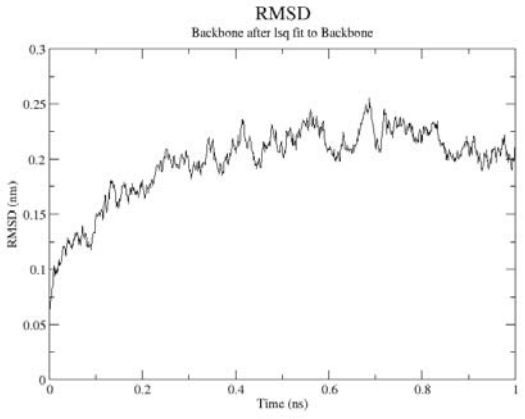

10667

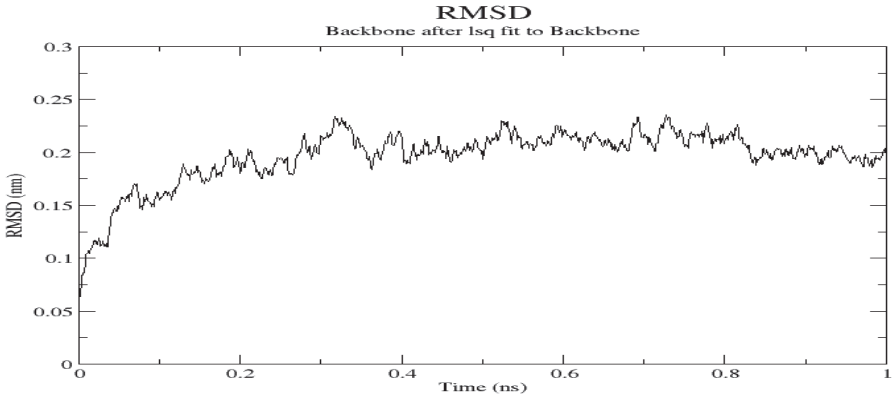

3175

Fig. 6b. Molecular dynamics simulation showing the RMSD plot of Naphthalene, 1-nitronaphthalene, 1-methylnaphthalene, 1,2-naphthoquinone and indomethacin towards COX

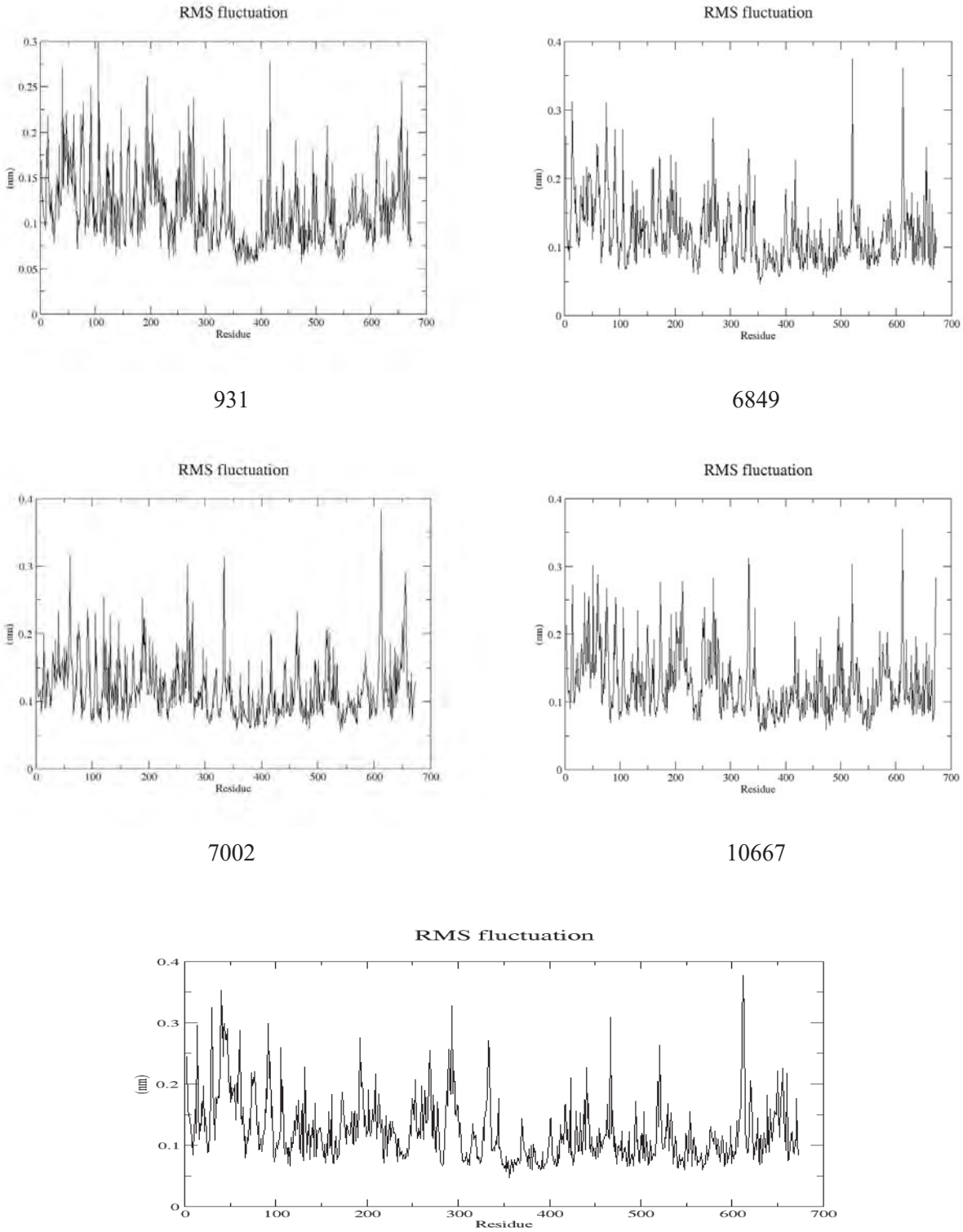

Fig. 6c. Molecular dynamics simulation showing the RMSF plot of Naphthalene, 1-nitronaphthalene, 1-methylnaphthalene, 1,2-naphthoquinone and indomethacin towards COX

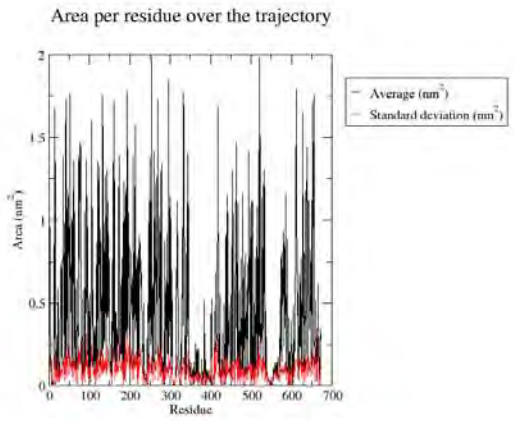

931

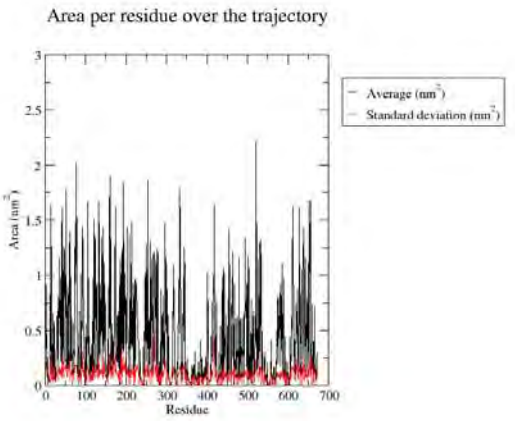

6849

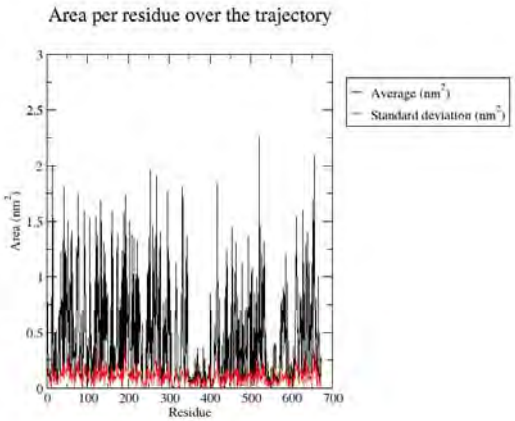

7002

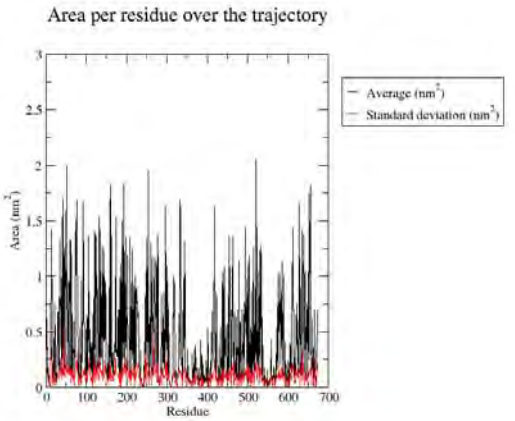

10667

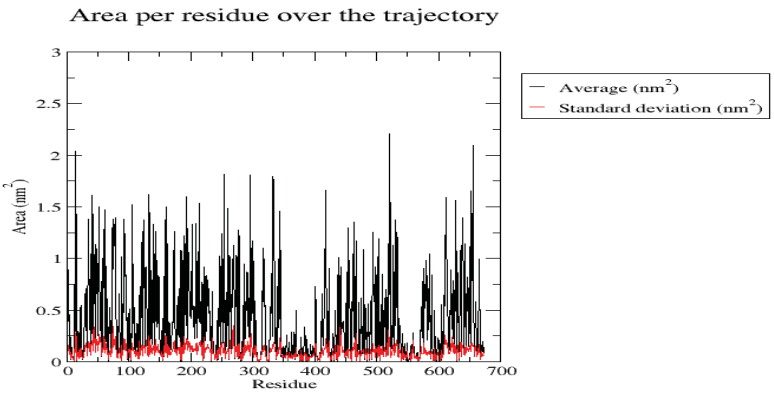

3175

Fig. 6d. Molecular dynamics simulation showing the area per residue of Naphthalene, 1-nitronaphthalene, 1-methylnaphthalene, 1,2-naphthoquinone and indomethacin towards COX

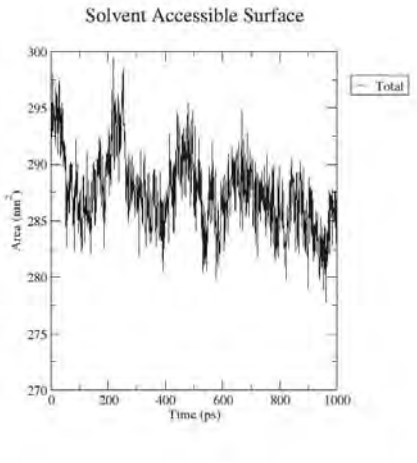

931

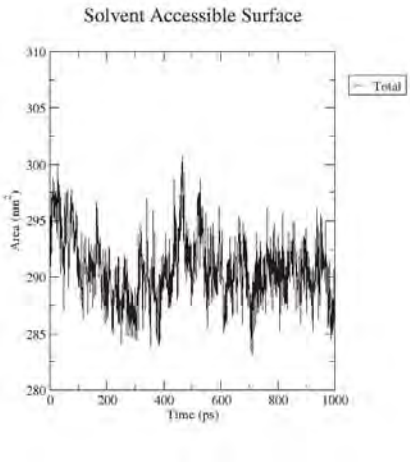

6849

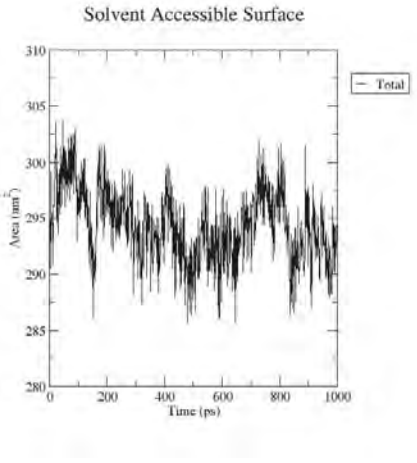

7002

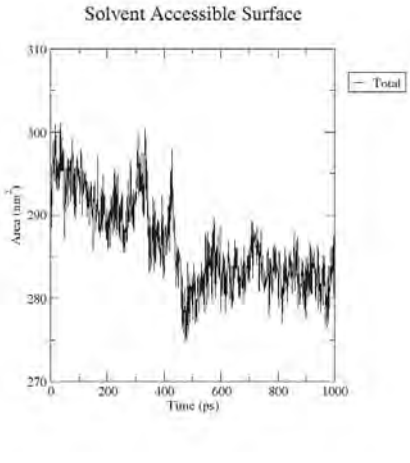

10667

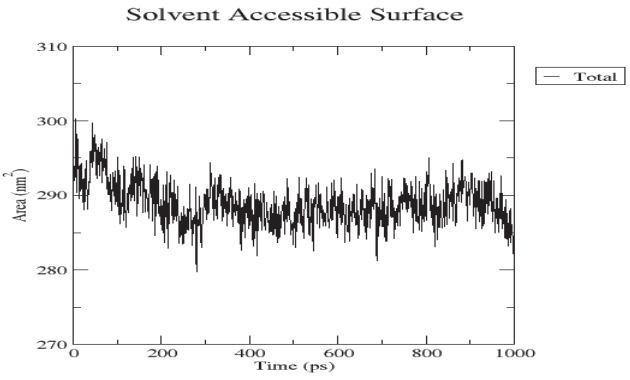

3175

Fig. 6e. Molecular dynamics simulation showing the SASA of Naphthalene, 1-nitronaphthalene, 1-methylnaphthalene, 1,2-naphthoquinone and indomethacin towards COX

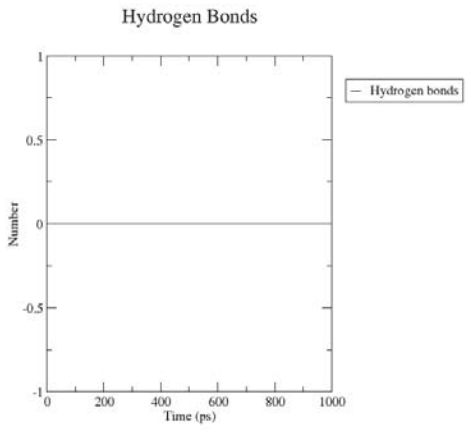

931

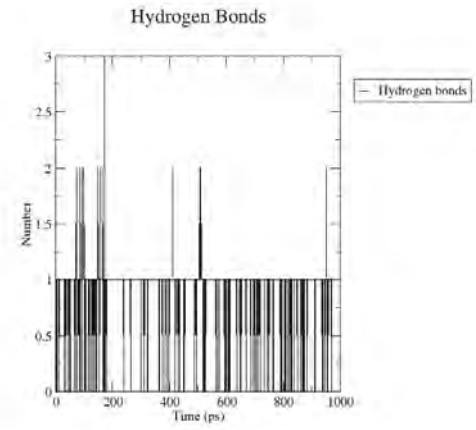

6849

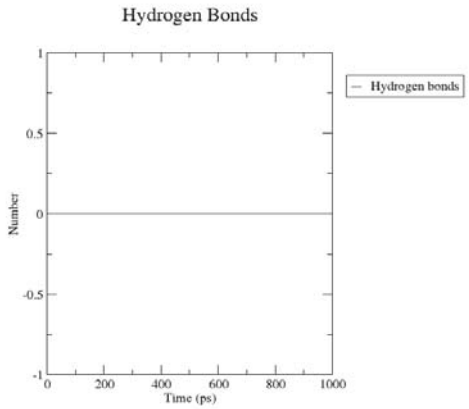

7002

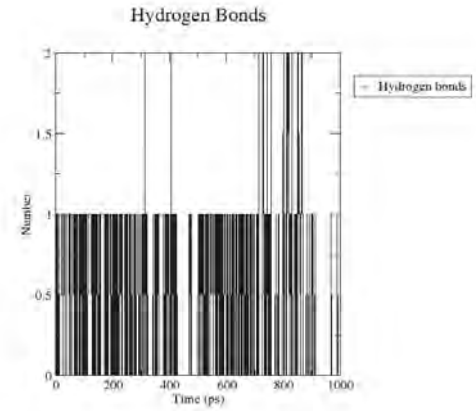

10667

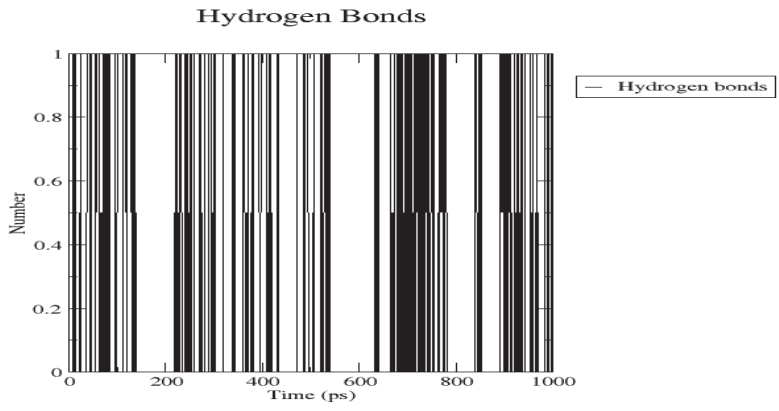

3175

Fig. 6f. Molecular dynamics simulation showing the Ligands Hydrogen bond of Naphthalene, 1-nitronaphthalene, 1-methylnaphthalene, 1,2-naphthoquinone and indomethacin towards COX

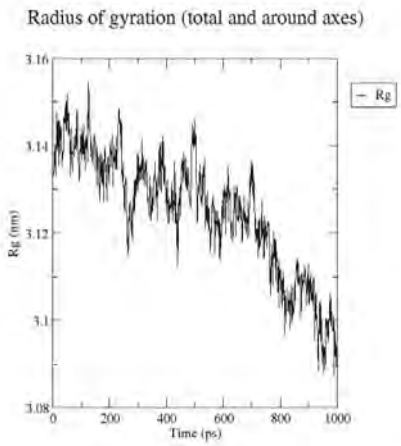

931

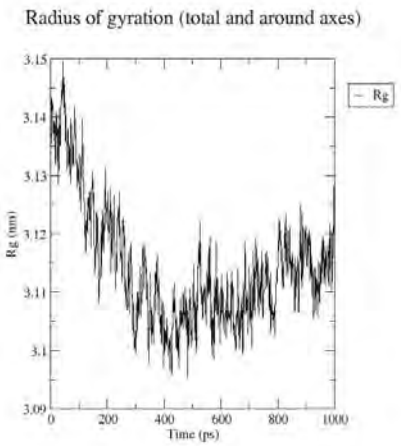

6849

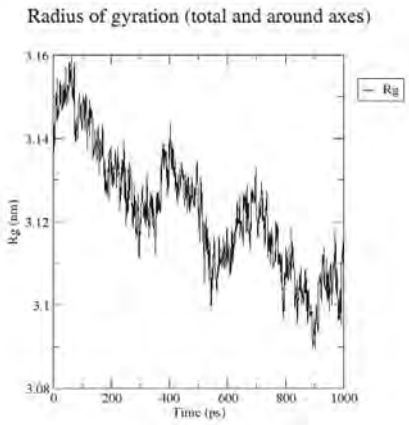

7002

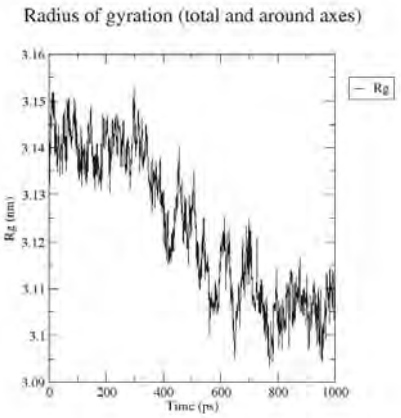

10667

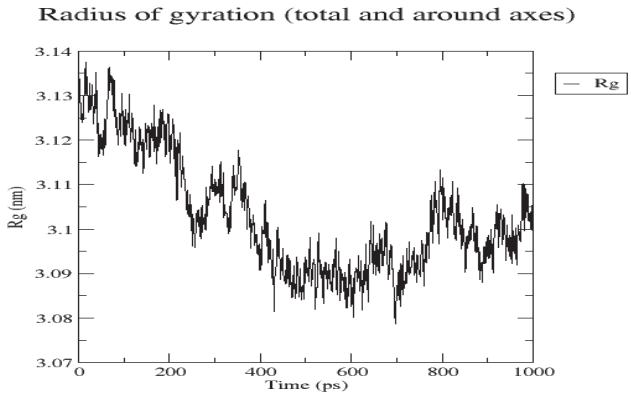

3175

Fig. 7a. Molecular dynamics simulation showing the Radius of gyration of Naphthalene, 1-nitronaphthalene, 1-methylnaphthalene, 1,2-naphthoquinone and indomethacin towards LOX

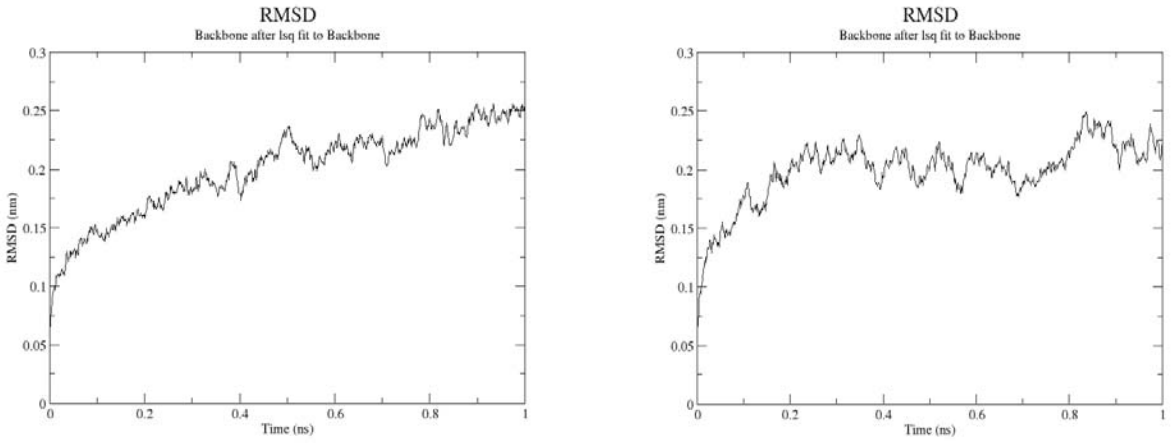

931

6849

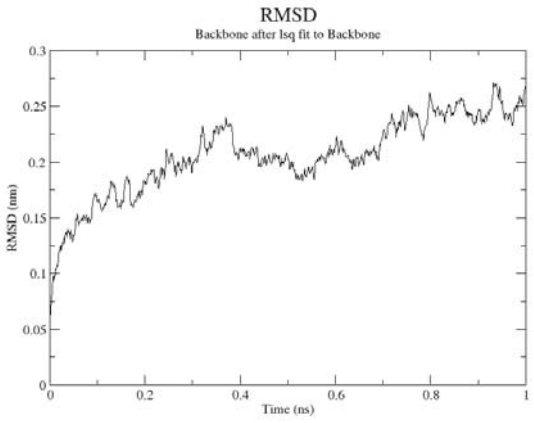

7002

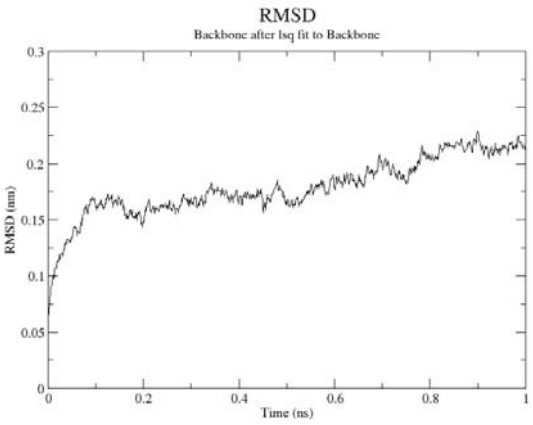

10667

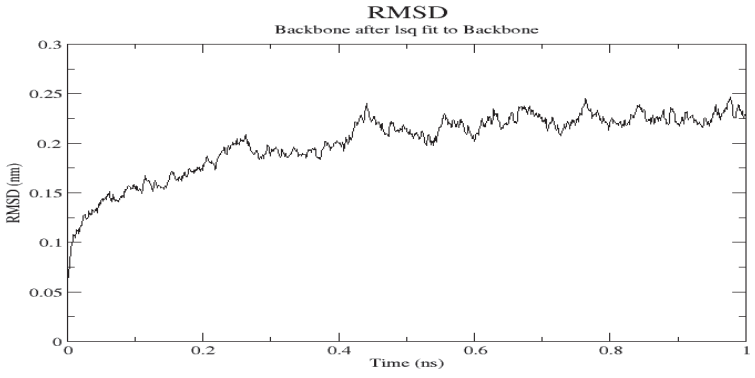

3175

Fig. 7b. Molecular dynamics simulation showing the RMSD plot of Naphthalene, 1-nitronaphthalene, 1-methylnaphthalene, 1,2-naphthoquinone and indomethacin towards LOX

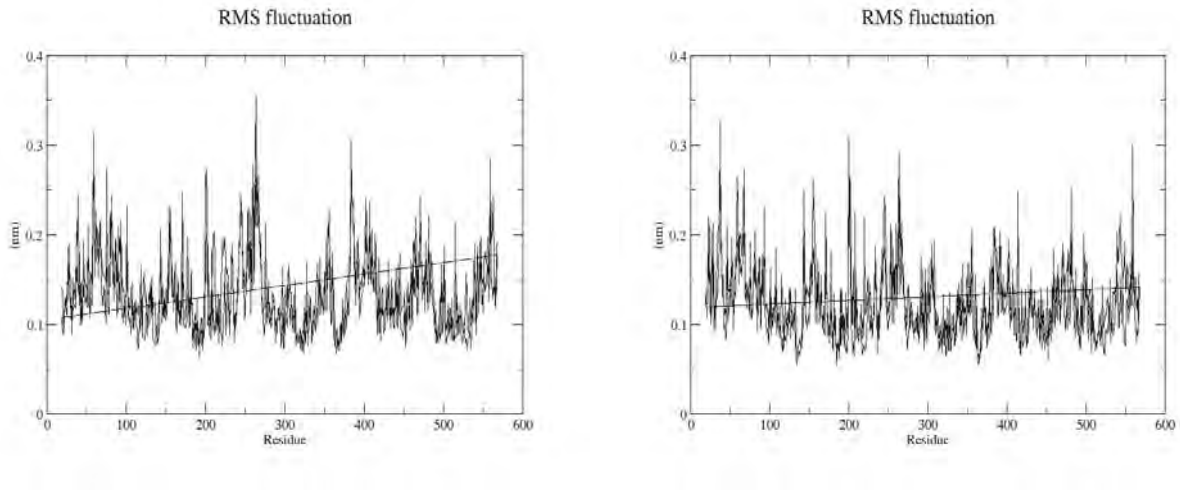

931

6849

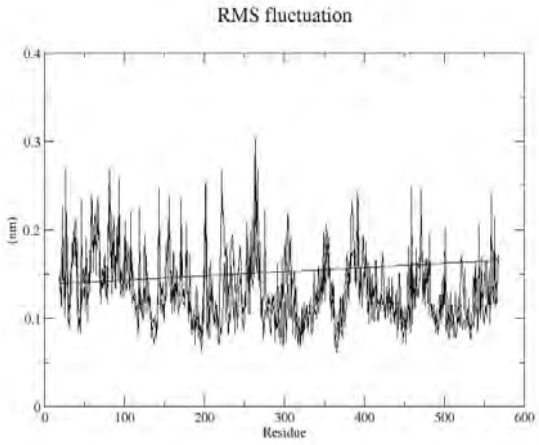

7002

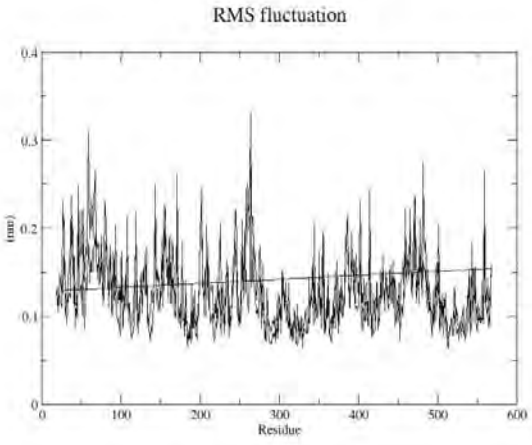

10667

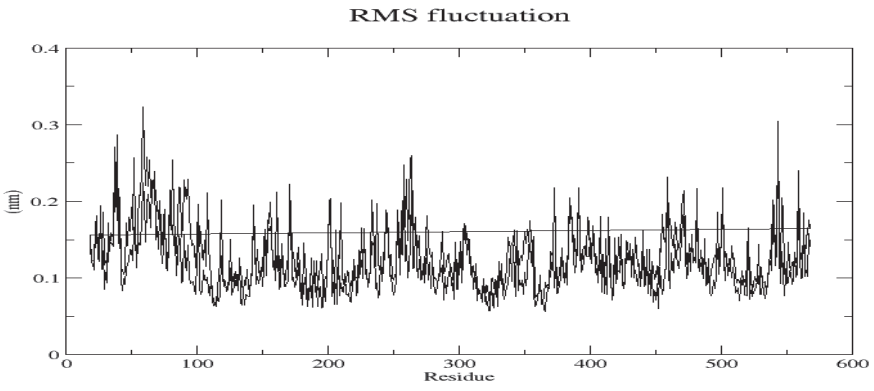

3175

Fig. 7c. Molecular dynamics simulation showing the RMSF plot of Naphthalene, 1-nitronaphthalene, 1-methylnaphthalene, 1,2-naphthoquinone and indomethacin towards LOX

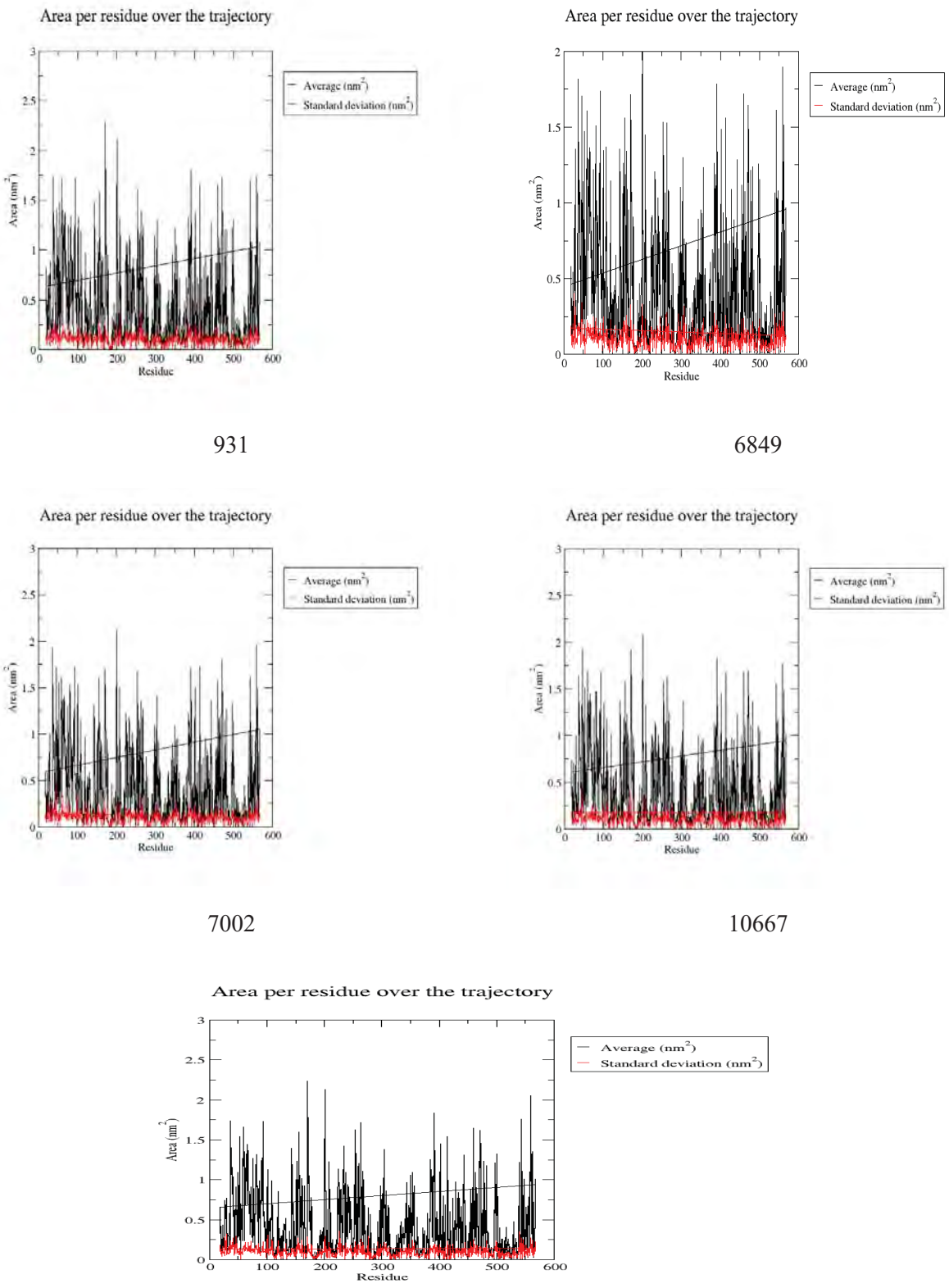

Fig. 7d. Molecular dynamics simulation showing the Area per residue of Naphthalene, 1-nitronaphthalene, 1-methylnaphthalene, 1,2-naphthoquinone and indomethacin towards LOX

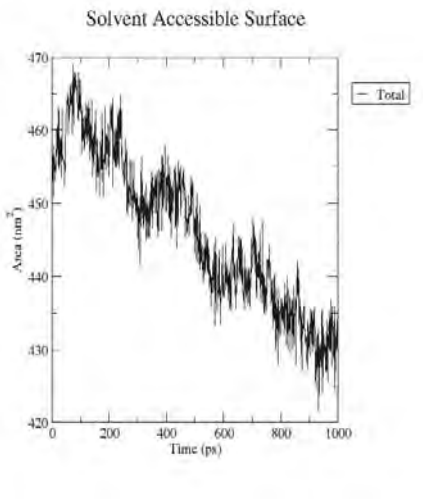

931

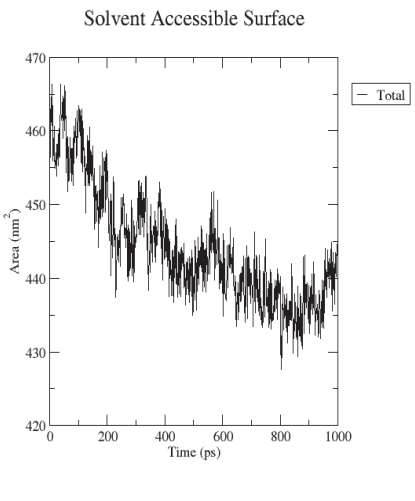

6849

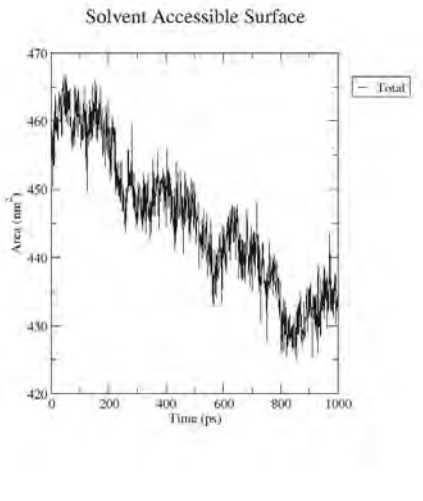

7002

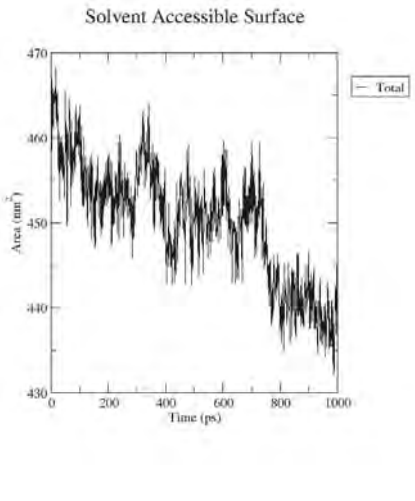

10667

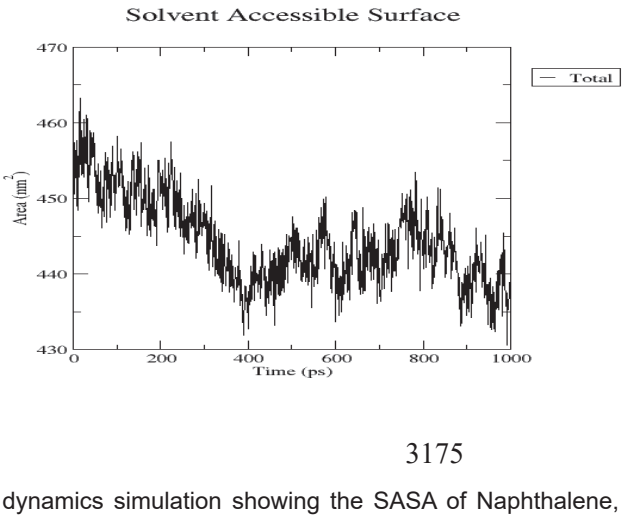

3175

Fig. 7e. Molecular dynamics simulation showing the SASA of Naphthalene, 1-nitronaphthalene, 1-methylnaphthalene, 1,2-naphthoquinone and indomethacin towards LOX

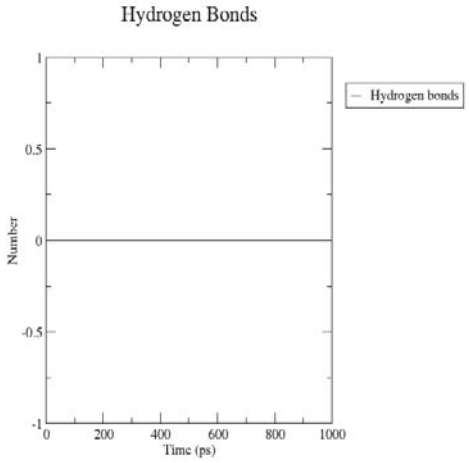

931

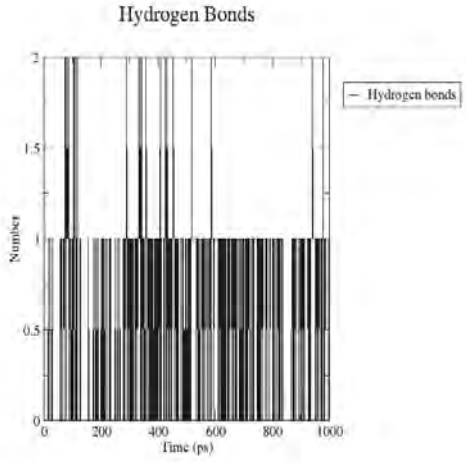

6849

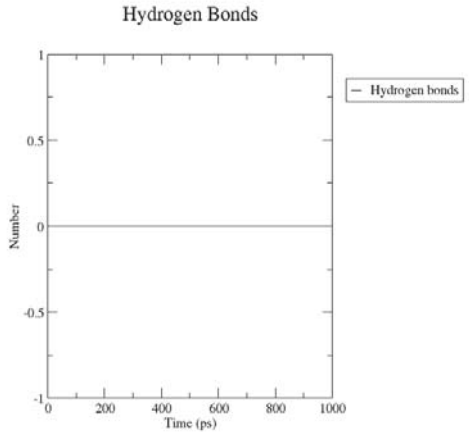

7002

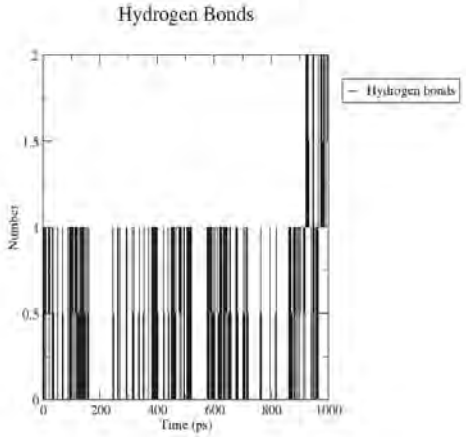

10667

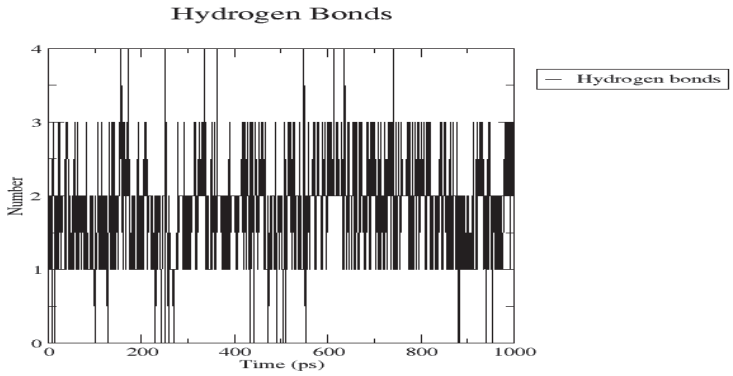

3175

Fig. 7f. Molecular dynamics simulation showing the Ligands Hydrogen bond of Naphthalene, 1-nitronaphthalene, 1-methylnaphthalene, 1,2-naphthoquinone and indomethacin towards COX

DISCUSSION

COX-2, a tissue-specific isoenzyme, plays a crucial role in inflammatory processes via the production of inflammatory prostaglandins, making them a suitable target for the development of nonsteroidal antiinflammatory drugs (NSAIDs) [20, 21, 22]. The release of MDA has been reported in several studies as a biomarker of antiinflammatory enzymes such as COX and LOX in the metabolism of eicosanoids. Hence, the release of this by-product was assessed and quantified. This study revealed a significant increase in serum MDA level during the first two hours of NA exposure, which occurred at the lower dose (0.75 g/m3) compared with the control. This result is in line with the earlier reported work on oxidative stress due to NA [23, 24, 25]. It is evident from Table 1 that the MDA level in the NA-exposed rat at a higher dose (1.50 g/m3) showed no significant difference compared to the control. This significant reduction in MDA level at higher doses could be due to adaptability potential from the animal [26] or faster glutathione turnover via upregulation of glutamate-cysteine ligase [27, 28]. Meanwhile, prolonged NA exposure resulted in a significant decrease in MDA release at all doses (Table 1) compared to the control, suggesting its analgesic potential via dephosphorylation of protein tyrosine kinase causing the inhibition of COX and LOX activities [29].

The swiss model GMQE scores of 0.95 and 0.88 of rat COX and LOX, respectively, while -1.02 and -0.57 obtained respectively for QMEAN scores (Figure 1) suggested a good quality, reliability and the degree of nativeness of the built models to the experimental structure of similar size that could be due to the close score values for respective GMQE (between 0 and 1) and QMEAN Z-score (between -4.0 and 0) for COX and LOX models [30, 31, 32]. In addition, the quality of the modeled protein structures was further assessed through the Ramachandran plot. The 90.9% and 91.9% values for residues in the favored region were obtained for COX and LOX, respectively, using PROCHECK, where a model with at least 90% Ramachandran summary plot value predicted good quality (Figures 2 and 3).

The molecular docking was carried out to clearly explain the mechanism of interactions for NA and its metabolites towards COX and LOX. The result of the study showed that all the ligands evaluated have a lower binding score than indomethacin except 1-nitronaphthalene, with a binding score of -7.07 kcal/mol, which is not significantly different from indomethacin. Also, all the assessed metabolites of NA showed better interaction towards COX, as seen in the binding scores, except 1,2-naphthoquinone, with insignificant binding scores compared to NA. This result supported our earlier report on 1,2-naphthoquinone poor interaction potential in NA metabolism [25]. It is evident from Table 2 that 1,2-naphthoquinone interacted with conventional hydrogen bonds but had the least binding score, which is not significantly different from NA. This low binding affinity from 1,2-naphthoquinone could be due to a low number of pi-bonds formation between 1,2-naphthoquinone and COX interacting residues [33, 34]. Also, Table 2 revealed that all metabolites of NA and NA interacted with similar residues: Met231, Tyr234 and Lys656, suggesting common pocket interaction towards COX except 1,2-naphthoquinone. This different binding site interaction could also be responsible for the low binding score exhibited by 1,2-naphthoquinone.

Conversely, indomethacin interaction with COX at another binding site with a high binding score could be due to a high number of pi-interactions as well as the conventional hydrogen bond (Figures 4a and 4b) [35]. Further assessment of NA analgesic potency was done on LOX. In an almost similar pattern where 1-nitronaphthalene showed the best binding score among NA metabolites, while 1,2-naphthoquinone had the least binding score (Table 3). However, all the ligands interacted at different sites except 1-methylnaphthalene and 1-nitronaphthalene with similar interacting residues (Ala188, Gln189 and His374), which could be responsible for the insignificant difference observed in their binding scores. The high binding scores observed in 1-nitronaphthalene and indomethacin could be attributed to the conventional hydrogen bond formation (Figure 5a and 5b), where both ligands served as the donor of most electrons for the formed interactions [35].

The effect of NA and its metabolites, as well as indomethacin, on the flexibility of prostaglandin synthetic enzymes (COX and LOX), was investigated by carrying out molecular dynamics simulation via radii of gyration, root mean square deviation (RMSD), root mean square fluctuation (RMSF), solvent accessible surface area (SASA), hydrogen bond etc. In molecular structures, the radii of gyration are fundamental for defining the root mean square distance from the center of the molecule [36, 37]. Interestingly, the Rg result depicted that all the metabolites of NA and indomethacin show Rg values greater than 2.80 nm within the first 200 ps except NA and 1,2-naphthoquinone with Rg values of 2.795 nm and 2.785 nm, respectively (Figure 6a). This could be responsible for the opening of the hydrophobic structure of the COX molecule [38], thus substantiating the low binding scores observed in NA and 1,2-naphthoquinone. However, Figure 7a showed that the Rg values reduce steadily in all the LOX-ligand complexes with respect to time progression except in NA and 1,2-naph-

thoquinone, where a sharp reduction was observed. Also, all the LOX-NA and its metabolites complexes showed a higher Rg value of 3.15 nm than the LOX-indomethacin complex in the first 100 ps.

Exploring RMSD with time progression defined the stability of the assessed COX and LOX [39]. The RMSD plot of COX-ligand complexes and LOX-ligand complexes depicted in Figure 6b and 7b, respectively, is based on all backbone Cα atoms relative to the corresponding starting structures with the time progression. The RMSD plot revealed that all the ligands examined, including indomethacin, showed a steady increase in RMSD value that is less than 0.25 nm throughout the simulation time, suggesting the stability of COX backbone starting from 0.1 ns till the end of the simulation [40, 41]. Meanwhile, COX-1,2-naphthoquinone showed an RMSD value greater than 0.25 nm between 0.6 ns and 0.7 ns. Captivatingly, this result buttressed the lowest binding score observed in 1,2-naphthoquinone towards COX (Table 2). In an almost similar pattern, the RMSD values increased progressively with time of progression in all the LOX-ligand complexes. However, in all the complexes examined, only the LOX-1,2-naphthoquinone complex showed an RMSD value less than 0.25 nm in the last 200 ns, correlating with the low binding score observed in the molecular docking study (Table 3). Also, the residue-specific flexibility was assessed by measuring the RMSF values on individual residues. It can be concluded from Figures 6c and 7c that none of the ligands investigated exceeded 0.375 nm and caused higher fluctuation of residues and their backbone atoms in COX and LOX, suggesting slight or no conformational changes during the simulation.

Furthermore, the SASA factor and area per residue were examined, and the result revealed that none of the COX-ligands complexes show significant differences in SASA, and deviation in the area per residue during simulation suggested no structural relaxation, thus no protein variability except 1,2-naphthoquinone-COX with standard deviation value greater than 0.5 nm2 [42, 43]. However, structural flexibility was observed in the LOX-ligand complexes due to a progressive decrease in SASA during the time course of progression, suggesting protein variability in all the examined complexes while the area per residue remained constant throughout the time of simulation (Figures 6d and 7d; 6e and 7e) [42, 43]. Lastly and surprisingly, the conventional hydrogen bond formation in the molecular dynamic simulations of all the ligands complexed with the examined enzymes supported the molecular docking result where no hydrogen bond formation occurred in NA and 1-methylnaphthalene interactions (Figures 6f and 7f).

CONCLUSIONS

The study suggested that NA reduced the synthesis of MDA in the in vivo work, which could be due to the inhibition of cyclooxygenase and lipoxygenase activities, where 1-nitronaphthalene showed the highest binding affinity in the *in silico* work.

Ethics approval and consent to participate: *Not applicable*

Consent for publication: *Not applicable*

Availability of data and materials: *All data generated or analyzed during this study are included in this published article.*

Competing of interests: *The authors declare that they have no conflict of interests*

Funding: *Not applicable*

Authors' contributions: *IO, GA, AA, BO, and OA conceived, designed, and performed the experiments, while AA and RB performed the experiment. The manuscript was written, proofread, and approved by the authors.*

Acknowledgments: *We acknowledge the support provided by the staff of the Department of Biochemistry, College of Natural and Applied Sciences, McPherson University, Seriki Sotayo, Ogun State, Nigeria, is well appreciated.*

REFERENCES

1. Jing M, Han G, Wan J et al. Catalase and superoxide dismutase response and the underlying molecular mechanism for naphthalene. Science of the Total Environment 736: 2020,139567. https://doi.org/10.1016/j.scitotenv.2020.139567
2. Stohs SJ, Ohia S, Bagchi D. Naphthalene toxicity and antioxidant nutrients. Toxicology 2002;180,(1):97-105. https://doi.org/10.1016/S0300-483X(02)00384-0
3. Yost EE, Galizia A, Kapraun DF Health Effects of Naphthalene Exposure: A Systematic Evidence Map and Analysis of Potential Considerations for Dose – Response Evaluation, 2021;129.
4. Abozeid MA, El-sawi AA, Abdelmoteleb M et al. Hybrids with potent antitumor, antiinflammatory, 2020,42998-43009. https://doi.org/10.1039/d0ra08526j
5. Pandya AB, Prajapati DG, Pandya SS. Synthesis of novel Naphthalene COX inhibitors for antiinflammatory activity. Journal of Applied Pharmaceutical Science 2012;2(8):226–232. https://doi.org/10.7324/JAPS.2012.2840
6. Sharma S, Singh T. A study of novel antiinflammatory derivatives of novel α-amino naphthalene and β-amino naphthalene. Archive de Pharmazie 2006;339,135-152.
7. Mohammed, MS, Osman WJA, Garelnabi EA et al. Secondary metabolites as antiinflammatory agents. The Journal of Phytopharmacology 2014;3(4): 275-285.
8. El haimeur B, Bouhallaoui M, Zbiry M et al. Use of biomarkers to evaluate the effects of environmental stressors on Mytilus galloprovincialis sampled along the Moroccan coasts: Integrating biological and chemical data. Marine Environmental Research 2017;130,60-68. https://doi.org/10.1016/j.marenvres.2017.05.010

9. Zhang F, Zhang Y, Wang K et al. Protective effect of diallyl trisulfide against naphthalene-induced oxidative stress and inflammatory damage in mice. International Journal of Immunopathology and Pharmacology 2016;29(2):205–216. https://doi.org/10.1177/0394632015627160
10. Buege JA, Aust SD. Microsomal lipid peroxidation. Methods Enzymol. 1978;52:302-10. doi: 10.1016/s0076-6879(78)52032-6
11. Trott O, Olson AJ. AutoDock Vina: Improving the speed and accuracy of docking with a new scoring function, efficient optimization and multithreading. Journal of Computational Chemistry, 2010;31(2): 455-461. https://doi.org/10.1002/jcc.21334
12. Kim S, Chen J, Cheng T et al. PubChem 2019 update: improved access to chemical data. Nucleic Acids Research. 2019;47 (D1): D1102–D1109. doi: 10.1093/nar/gky1033
13. The UniProt Consortium. UniProt: the universal protein knowledgebase in 2021. Nucleic Acids Research, 2021;49(D1): D480-D489. https://doi.org/10.1093/nar/gkaa1100
14. Waterhouse A, Bertoni M, Bienert S et al. () SWISS-MODEL: homology modelling of protein structures and complexes. Nucleic Acids Res. 2018;46(W1): W296-W303. https://doi.org/10.1093/nar/gky427
15. Laskowski RA, MacArthur MW, Moss DS, Thornton JM () PROCHECK: a program to check the stereochemical quality of protein structures. J. Appl Crystal 1993;26(2):283-291. https://doi.org/10.1107/S0021889892009944
16. Laskowski RA, Rullmannn JA, MacArthur MW et al. AQUA and PROCHECK-NMR: programs for checking the quality of protein structures solved by NMR. J Biomol NMR 1996;8(4): 477-486. https://doi.org/10.1 007/BF00228148
17. Schüttelkopf AW, van Aalten DMF. PRODRG: a tool for high-throughput crystallography of protein-ligand complexes. Acta Crystallogr 2004,D60, 1355-1363.
18. Bekker H, Berendsen HJC, Dijkstra EJ et al. Gromacs: A parallel computer for molecular dynamics simulations" 252–256 in Physics computing 92. Edited by R.A. de Groot and J. Nadrchal. World Scientific, Singapore, 1993.
19. Abraham MJ, Murtola T, Schulz R et al. GROMACS: High performance molecular simulations through multi-level parallelism from laptops to supercomputers, SoftwareX, 2015, 1-2 19-25.
20. Singh P, Mittal A. Current status of COX-2 inhibitors. Mini Rev Med Chem. 2008;8(1):73-90
21. Rouzer CA, Marnett LJ. Cyclooxygenases: structural and functional insights. J Lipid Res. 2009;50,S29-34. 10.1194/jlr.R800042-JLR200
22. Chakraborti AK, Garg SK, Kumar R et al. Progress in COX-2 inhibitors: a journey so far. Curr Med Chem. 2010;17(15):1563-1593.
23. Baldwin RM, Jewell WT, Fanucchi MV et al, Comparison of pulmonary/nasal CYP2F expression levels in rodents and rhesus macaque. J Pharmacol Exp Therapy 2004;309,127-136
24. Kushwah DS, Salman MT, Singh P et al. Protective effects of ethanolic extract of Nigella sativa seed in paracetamol induced acute hepatotoxicity in vivo Pak J Biol Sci 2014;17(4):517-22. doi: 10.3923/pjbs.2014.517.522.
25. Olaoye I, Awotula A, Oso B et al. Naphthalene exposure decreases reduced glutathione in male Wistar rats. Biotecnol Apl. 2022;39(1):1201-10.
26. West JA, Pakehham G, Morin D et al. Inhaled naphthalene causes dose dependent Clara cell cytotoxicity in mice but not in rats. Toxicol Appl Pharmacol 2001;173(2):114-9. doi: 10.1006/taap.2001.9151
27. West JA, Buckpitt AR, Plopper CG. Elevated airway GSH resynthesis confers protection to Clara cells from naphthalene injury in mice made tolerant by repeated exposures. Journal of Pharmacology and Experimental Therapeutics 2000;294,516-523.
28. West JA, Williams KJ, Toskala E et al. Induction of tolerance to naphthalene in Clara cells is dependent on a stable phenotypic adaptation favoring maintenance of the glutathione pool. Am J Pathol 2002;160(3):1115-27. doi: 10.1016/S0002-9440(10)64932-2
29. Kikuno S, Taguchi K, Iwamoto N et al. 1,2-Naphthoquinone activates vanilloid receptor 1 through increased protein tyrosine phosphorylation, leading to contraction of guinea pig trachea. Toxicol Appl Pharmacol 2006;210,47-54.
30. Benkert P, Biasini M, Schwede T. Toward the estimation of the absolute quality of individual protein structure models, Bioinformatics 2011;27(3):343-350. https://doi.org/10.1093/bioinformatics/btq662
31. Cardoso JM, Fonseca L, Egas C, Abrantes I. Cysteine proteases secreted by the pinewood nematode, Bursaphelenchus xylophilus: *in silico* analysis. Comput Biol Chem. 2018;77,291-296
32. Patel B, Singh V, Patel D. Structural Bioinformatics. In: Shaik NA, Hakeem, KR, Banaganapalli, B, Elango, R. editors. Essentials of Bioinformatics, vol. I. Cham, Switzerland: Springer 2019,169-199. https://doi.org/10.1007/978-3-030-02634-9
33. Brylinski M. Aromatic interactions at the ligand-protein interface: Implications for the development of docking scoring functions. Chem Biol Drug Des 2018;91(2):380- 90.
34. Olaoye I, Oso B, Aberuagba A. Molecular Mechanisms of Anti-Inflammatory Activities of the Extracts of Ocimum gratissimum and Thymus vulgaris. Avicenna Journal of Medical Biotechnology 2021;13(4):207-216 http://dx.doi.org/10.18502/ajmb.v13i4.7206
35. Elokely KM, Doerksen RJ. Docking challenge: protein sampling and molecular docking performance. J Chem Inf Model 2013;53(8):1934-5
36. Tanner JJ. Empirical power laws for the radii of gyration of protein oligomers. Acta Cryst D72:2016,1119-1129. http://dx.doi.org/10.1107/S2059798316013218
37. Shukla R, Shukla H, Kalita P, Tripathi T. Structural insights into natural compounds as inhibitors of Fasciola gigantica thioredoxin glutathione reductase. J Cell Biochem. 2017,1-32. 10.1002/jcb.26444
38. Adewole K, Adebayo I, Olaoye I. *In silico* profiling of histone deacetylase inhibitory activity of compounds isolated from Cajanus cajan. Beni-Suef Univ J Basic Appl Sci 2022;11,9. https://doi.org/10.1186/s43088-021-00191-y
39. Maiorov VN, Crippen GM. Significance of root mean-square deviation in comparing three-dimensional structures of globular proteins. Journal of Molecular Biology 1994;235,625-634. doi:10.1006/jmbi.1994.1017
40. Martinez L. Automatic identification of mobile and rigid substructures in molecular dynamics simulations and fractional structural fluctuation analysis. PLoS ONE 2015;10(3):e0119264. https://doi.org/10.1371/journal. pone.0119264
41. Sargsyan K, Grauffel C, Lim C. How molecular size impacts RMSD applications in molecular dynamics simulations. J Chem Theory Comput. 2017;13(4):1518-1524. https://doi.org/10.1021/acs.jctc.7b00028
42. Mattea C, Qvist J, Halle B. Dynamics at the protein-water interface from 17O spin relaxation in deeply supercooled solutions. Biophys J. 2008;95(6):2951-63.
43. Damjanović A, Brooks BR, Garcia-Moreno´ BE. Conformational relaxation and water penetration coupled to ionization of internal groups in proteins. J Phys Chem 2011;115(16):4042-53